Past and future simulations of NO2 from a coupled chemistry-climate model in comparison with observations

H. Struthers, K. Kreher, J. Austin, R. Schofield, G. Bodeker, P. Johnston, H. Shiona, A. Thomas

**Atmospheric
Chemistry
and Physics
Discussions**

ACPD

4, 4545–4579, 2004

Past and future NO$_2$

H. Struthers et al.

Title Page

Abstract	Introduction
Conclusions	References
Tables	Figures

◄◄	►►
◄	►
Back	Close

Full Screen / Esc

Print Version

Interactive Discussion

© EGU 2004

Past and future simulations of NO$_2$ from a coupled chemistry-climate model in comparison with observations

H. Struthers[1], K. Kreher[1], J. Austin[2], R. Schofield[3], G. Bodeker[1], P. Johnston[1], H. Shiona[1], and A. Thomas[1]

[1]National Institute of Water and Atmospheric Research, Private Bag 50061, Omakau, New Zealand
[2]Geophysical Fluid Dynamics Laboratory, Princeton Forrestal Campus Rte.1, 201 Forrestal Rd., Princeton, NJ 08542-0308, USA
[3]NOAA Aeronomy Laboratory, 325 Broadway, R/AL8, Boulder CO 80305, USA
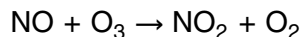
Correspondence to: H. Struthers (h.struthers@niwa.co.nz)

Abstract

Trends in NO_2 derived from a 45 year integration of a chemistry-climate model (CCM) run have been compared with ground-based NO_2 measurements at Lauder (45° S) and Arrival Heights (78° S). Observed trends in NO_2 at both sites exceed the trends in N_2O, the primary source gas for stratospheric NO_2, suggesting that processes driving the NO_2 trend are more complex than direct conversion of N_2O to NO_2. If CCMs are to accurately estimate future changes in ozone, it is important that they comprehensively include these $N_2O \rightarrow NO_2$ processes since NO_x ($NO+NO_2$) concentrations are an important factor affecting ozone concentrations. Comparison of measured and modelled NO_2 trends is a sensitive test of the degree to which these processes are incorporated in the CCM used here. At Lauder the 1980–2000 CCM NO_2 trends (4.2% per decade at sunrise, 3.9% per decade at sunset) are lower than the observed trends (6.5% per decade at sunrise, 6.0% per decade at sunset) but not significantly different at the 2σ level. Large variability in both the model and measurement data from Arrival Heights makes trend analysis of the data difficult. CCM predictions (2001–2019) of NO_2 at Lauder and Arrival Heights show significant reductions in the rate of increase of NO_2 compared with the previous 20 years (1980–2000). The model results indicate that the partitioning of oxides of nitrogen changes with time and is influenced by both chemical forcing and circulation changes.

1. Introduction

It has been recognised for some time that the reactive species NO_x are important in the altitude range from approximately 20 km to 35 km in determining the concentration of stratospheric ozone (Crutzen, 1970). NO_x destroys ozone through the catalytic cycle shown in Reactions (R1) and (R2).

$$NO + O_3 \rightarrow NO_2 + O_2 \tag{R1}$$

$$NO_2 + O \rightarrow NO + O_2 \qquad \text{(R2)}$$

$$\text{(net)} \quad O_3 + O \rightarrow 2\,O_2 \qquad \text{(R3)}$$

In the lower stratosphere (approximately 10 km to 20 km) the most significant influence of NO_x is its interaction with the ClO_x and BrO_x ozone loss cycles via the formation of reservoir species $ClONO_2$ and $BrONO_2$. NO_2 also reacts with OH (Eq. R4), reducing the HO_x concentration and thus inhibiting the HO_x catalysed destruction of ozone.

$$NO_2 + OH + M \rightarrow HNO_3 + M. \qquad \text{(R4)}$$

The major source of stratospheric NO_x is oxidation of N_2O (Minschwener et al., 1993).

$$N_2O + O(^1D) \rightarrow 2NO. \qquad \text{(R5)}$$

N_2O concentrations are predicted to continue to increase over the coming century due to anthropogenic surface emissions, mostly attributed to agricultural nitrogen fixation (IPCC, 2001; WMO, 1999). Trends in the concentration of atmospheric N_2O for the period 1980 to 1988 have been estimated to be +0.25±0.05% per year (IPCC (2001), p253). Zander et al. (1994) quote a trend in N_2O of +0.33±0.04 % per year based on remote measurements made at Jungfraujoch from 1984 to 1996. In contrast to N_2O, stratospheric halogen concentrations are expected to decline over the coming 50 years as anthropogenic emissions of halogenated ozone-depleting compounds decrease (WMO, 2003). It is therefore important to understand the combined effect of changing halogen and NO_x concentrations on the future evolution of the ozone layer.

Randeniya et al. (2002) studied the effect of increasing N_2O and methane on northern mid-latitude ozone columns for the period 2000–2100 using the CSIRO two dimensional chemical model (Randeniya et al., 1997). Their model results show partial recovery of ozone columns through to the middle of the century due to reductions in halogen concentrations. This is followed by reduction in ozone columns from 2050 to 2100 which Randeniya et al. (2002) attribute to increased destruction of ozone by NO_x,

Past and future NO2

H. Struthers et al.

modulated by the amount of methane present in the model. Methane concentrations influence the ozone recovery through the photo-oxidation of methane by halogen radicals in the lower stratosphere and above 20 km through changes in OH concentrations leading to changes in the rate of conversion of NO_2 to HNO_3. Comparing model ozone profiles for 2100 with profiles from 2000, Randeniya et al. (2002) find increases in lower stratospheric ozone concentrations over the 2000–2100 integration. This is explained by a reduction in the amount of ozone destroyed by halogen catalytic cycles. However, the recovery in lower stratospheric ozone is offset by reductions of up to 7% in ozone concentrations in the middle stratosphere due to increased NO_x catalytic destruction of ozone.

Modelling future ozone change requires realistic representations of the anticipated changes in NO_x and halogens, in addition to the many other interacting chemical and dynamical components of the stratospheric system. Three-dimensional coupled chemistry-climate models (CCMs) are designed to capture the interaction between climate change and changes in atmospheric chemistry and are now becoming important tools in the prediction of future stratospheric chemistry and dynamics (WMO, 2003). To have confidence in CCM predictions of future stratospheric change, it is necessary to assess their reliability. An important methodology for validating components of atmospheric chemical models is comparison of long time-series of modelled and measured amounts of trace gases.

Since climate models underpinning all CCMs are chaotic and exhibit unforced variability, comparisons of CCM output with observations are necessarily statistical in nature. Although comparisons between CCM output and observations on individual days are not meaningful in anything other than a climatological sense, the response of the model to long term forcings should agree with the response observed in the real atmosphere. For this reason, long time-series of observations are required to compare the modelled response to atmospheric forcings (WMO, 2003).

High quality measurements of NO_2 slant column densities have been routinely made at Lauder, New Zealand (45° S) since 1980 (Johnston and McKenzie, 1989) and Ar-

ACPD

4, 4545–4579, 2004

Past and future NO$_2$

H. Struthers et al.

Title Page

Abstract | Introduction

Conclusions | References

Tables | Figures

◄ | ►

◄ | ►

Back | Close

Full Screen / Esc

Print Version

Interactive Discussion

rival Heights, Antarctica (77.8° S) since 1982 (McKenzie and Johnston, 1984; Keys and Johnston, 1986, 1988). The measurements are taken at twilight (sunrise and sunset). Measuring at a solar zenith angle (SZA) of 90° with zenith sky viewing geometry increases the sensitivity of the observed columns to stratospheric NO_2 amounts (Solomon et al., 1987).

Liley et al. (2000) studied the Lauder NO_2 data set using least squares regression. Indices of QBO, ENSO, solar cycle and the El Chichon and Pinatubo volcanic events in addition to the NO_2 annual cycle and secular trend were fitted to the measured NO_2 time-series. Liley et al. (2000) concluded that the mean 90° SZA linear trend in NO_2 over Lauder from 1980 to 1999 was 5±1% per decade (sunrise trend 5.9±2.4, sunset trend 4.6±1.5 % per decade). These trends are significantly greater than the trend in N_2O estimated to be between 2.5% and 3.3% per decade (WMO, 1999). As N_2O is the dominant source of stratospheric NO_2, this result implies that there has been a dynamical or chemical change at southern mid-latitudes which has increased NO_2 disproportionately.

Using 1995–2002 Fourier Transform Infra-Red (FTIR) measurements at Kitt Peak (31.9° N), Rinsland et al. (2003) derived an NO_2 trend of 10.3±5.5% (2σ) per decade. However, the short time period used (8 years) resulted in large uncertainties on their trend (Liley et al., 2000) and their results cannot be meaningfully compared with those of Liley et al. (2000) or those presented here. NO_2 data derived from a combination of FTIR and differential optical absorption spectroscopy measurements taken at the Network of the Detection of Stratospheric Change (NDSC) station at Jungfrauoch (46.5° N) have been analysed and suggest a linear increase for the period 1985–2001 of 6±2% per decade (WMO, 2003). These results suggest that the NO_2 trend being greater than the N_2O trend is unlikely to be a local feature at Lauder but is likely to be of global extent.

Fish et al. (2000) used a column model to determine the sensitivity of southern mid-latitude NO_2 to changes in stratospheric temperature, ozone and water vapour. A number of possible mechanisms that could change the amount of NO_2 relative to the

Title Page

Abstract | Introduction

Conclusions | References

Tables | Figures

◄◄ | ►►

◄ | ►

Back | Close

Full Screen / Esc

Print Version

Interactive Discussion

© EGU 2004

amount of N_2O were identified:

- direct emission of NO_x

- changes in stratospheric circulation

- changes in the shape of the mean NO_2 profile

5   - changes in the partitioning of NO_y ($NO + NO_2 + NO_3 + HNO_3 + 2N_2O_5 + HNO_4 + ClONO_2 + BrONO_2$).

Changes in the partitioning of NO_y could arise due to changes in ozone, temperature, stratospheric water vapour and sulfate aerosol. The focus of Fish et al. (2000) was to determine whether changes in the partitioning of NO_y could explain the observed trend 10   in NO_2. The model was forced with observed changes in ozone, temperature and water vapour and a 2.5% per decade increase in N_2O. The model failed to reproduce the observed NO_2 trend (model trends +4.0±0.6% per decade at sunrise, +2.0±0.4% per decade at sunset). Including a 20% decrease in stratospheric aerosol in the model forcing gave NO_2 trends in agreement with observations (model trends +5.9±0.6% per 15   decade at sunrise, +4.3±0.4% per decade at sunset).

McLinden et al. (2001) used a combination of a three-dimensional chemical transport model, a static column chemistry model and a radiative transfer model to generate NO_2 slant column densities and compared the change in the columns over a 20 year time period with the Lauder NO_2 observations. Their results show a trend in NO_2 of 4.3% 20   per decade for a prescribed increase in N_2O of 3% per decade. Differences in the trends of NO_2 and N_2O were attributed to the less than equivalent conversion of N_2O to NO_y and repartitioning of NO_y due to ozone and halogen changes. The sensitivity of their system to temperature and aerosol changes was also investigated. McLinden et al. (2001) show that the trend in NO_2 vertical column density varies diurnally with 25   large changes in the slant column density trends at sunrise and sunset.

Both the studies of Fish et al. (2000) and McLinden et al. (2001) do not explicitly model the influence of circulation changes on NO_2 amounts. They use rather different

Past and future NO_2

H. Struthers et al.

Title Page

Abstract | Introduction

Conclusions | References

Tables | Figures

◄ | ►►

◄ | ►

Back | Close

Full Screen / Esc

Print Version

Interactive Discussion

models and forcings to estimate NO_2 slant column density trends. Both conclude that their models reproduce the observed NO_2 trend but differ in their conclusion as to why there is a distinction between the trends in NO_2 and N_2O. More work is required to fully understand the mechanisms responsible for the observed difference in trends.

5   In this paper we calculate NO_2 slant column densities for Lauder and Arrival Heights using results from the Unified Model with Eulerian Transport and Chemistry (UMETRAC), a three-dimensional CCM. NO_2 values are derived from a 40 year simulation of the model, (1980 to 2019). Model NO_2 slant columns for Lauder and Arrival Heights are compared with the measurements for the period 1980 to 2000 to test the model's

10   ability to reproduce the greater than than proportional increase in NO_2 relative to N_2O that has been observed in the measurements. The UMETRAC predictions of NO_2 trends at Lauder and Arrival Heights for the period 2001 to 2019 are introduced and discussed in light of the 1980 to 2000 model/observation comparison.

2. Measurements

15   The NO_2 measurement technique and retrieval algorithm are discussed by Johnston and McKenzie (1989) and Liley et al. (2000). The automated scanning spectrometers measure wavelengths from 435 nm to 450 nm with a spectral resolution of 1.2 nm. Twilight spectra are ratioed with midday reference spectra to remove Fraunhofer absorption lines present in sunlight. Each twilight measurement is also corrected for the

20   Ring effect (Grainger and Ring, 1963) using the "offset Ring" approach (Johnston and McKenzie, 1989).

The instruments at Lauder and Arrival Heights have been calibrated and intercompared to the standard required of the Network for Detection of Stratospheric Change (NDSC).

25   Model ozone and 20 hPa temperatures are also compared with measurements as changes in these quantities have been identified by Fish et al. (2000) and McLinden et al. (2001) as being important in determining changes in NO_2. The 20 hPa level

Past and future NO$_2$

H. Struthers et al.

Title Page

Abstract   Introduction

Conclusions   References

Tables   Figures

◄   ►

◄   ►

Back   Close

Full Screen / Esc

Print Version

Interactive Discussion

approximately coincides with the peak in the NO_2 mixing ratio and was therefore used as the level for the temperature comparison. It has been shown (Keys and Johnston, 1986) that NO_2 slant columns measured over Arrival Heights correlate strongly with stratospheric temperatures.

5 Modelled ozone data are compared with the NIWA assimilated ozone data-set (Bodeker et al., 2001). This data-set contains total column ozone values derived from a combination of TOMS and GOME satellite measurements which are corrected using ground-based network of Dobson spectrophotometers. NCEP/NCAR (Kalnay et al., 1996) 20 hPa temperature data are used for the temperature comparison.

10 **3.   Least squares regression analysis**

Linear trends in the NO_2 slant column density time-series are calculated using a least squares regression model (Bodeker et al., 2001). The regression model has been applied to ozone time-series in previous studies (Bodeker et al., 1998, 2001).

A number of forcings are known to influence the southern mid-latitude stratosphere:

15 – El Niño southern oscillation (ENSO)

– Quasi-biennial oscillation (QBO)

– 11 year solar cycle

– Volcanic injection of sulfate aerosol. For the time period 1980–2000, two volcanic events occurred which were significant for the southern mid-latitude stratosphere,
20 El Chichon (1982) and Pinatubo (1991).

The regression model is designed to allow fitting of indices for the above forcings, in addition to fitting the seasonal cycle and linear trend in the data. Inclusion of additional, higher order Fourier components to the basis describing the trend allows the model to fit seasonally varying trends in the data. Description of indices for the externally forced

Title Page

Abstract	Introduction
Conclusions	References
Tables	Figures

◄◄   ►►

◄   ►

Back   Close

Full Screen / Esc

Print Version

Interactive Discussion

basis functions (ENSO, QBO, solar cycle and volcanoes) within the regression model is given in Bodeker et al. (1998).

An autocorrelation model is also applied to the residual terms to ensure that uncertainties in the derived regression model parameters are estimated correctly.

⁵ For the observational record, all basis functions (ENSO, QBO, solar cycle volcanoes) are included in the regression analysis. For the model time-series, only the ENSO term is applied (in addition to the annual cycle (offset) and linear trend). The model does not include an 11 year solar cycle and uses an invariant, background sulfate aerosol field. The non-orographic gravity wave forcing scheme produces a QBO in the tropical
¹⁰ zonal winds (Scaife et al., 2000) that is produced internally within the climate model. This means that the model QBO is not correlated with observed QBO indices and so is not used in the regression analysis of the model data.

4. Model description

4.1. The coupled chemistry-climate model

¹⁵ UMETRAC uses the Met Office's Unified Model (UM) (Cullen and Davies, 1991) as the underlying climate model. The UM has been used in the Intergovernmental Panel on Climate Change assessments (e.g. IPCC, 2001). The model has a resolution of 3.75° (longitude), 2.5° (latitude) and 64 vertical levels from the surface to 0.01 hPa. A non-orographic gravity wave forcing scheme (Warner and McIntyre, 1999) is used to
²⁰ parameterise gravity wave breaking.

The UMETRAC chemistry scheme is based on a families approach (Austin, 1991). 15 chemical tracers and one dynamical tracer are advected by the model. The dynamical tracer is used to parameterise the long lived species H_2O, CH_4, Cl_y, Br_y, H_2SO_4 and NO_y. The chemistry scheme includes 65 gas phase chemical reactions, 9 het-
²⁵ erogeneous chemical reactions and 27 photolysis reactions. A PSC scheme based on liquid ternary solutions and water ice and a simple sedimentation scheme are also part

Full Screen / Esc

Print Version

Interactive Discussion

of the model. Chemical reaction rates are taken from DeMore et al. (1997) and Sander et al. (2000).

There are some differences between the UMETRAC configuration used in this paper and the configuration used in previous work (Austin and Butchart, 2003). These include a new tracer advection scheme, the chemistry scheme being applied over the whole vertical domain of the model rather than being restricted to the stratosphere and lower mesosphere, two additional chemical tracers are included (CO and CH_3OOH) and an extension of the chemical reaction set.

Water vapour concentrations in the chemistry module were taken from the UARS reference atmosphere project (URAP) reference atmosphere (http://code916.gsfc.nasa.gov/Public/Analysis/UARS/urap/home.html) and held fixed over the integration. The water vapour in the chemistry module is distinct from the water vapour modelled in the climate model to avoid problems with the sedimentation of PSCs. Stratospheric aerosol was derived from the aerosol surface area densities given in Table 8.8 of WMO (1991). Again, the aerosol amounts were held constant over the model integration.

Importantly for this study, the rate of increase of N_2O was fixed at +2.6% per decade for the entire length of the integration (1980 to 2019). The model uses a parameterisation to determine the amount of NO_y present at each time step, based on the transport of a conserved tracer and the compact relationships of Plumb and Ko. (1992). In a subsequent step, the model partitions the NO_y according to the chemical scheme within the model. The global rate of increase NO_y is fixed to the rate of increase in N_2O (2.6% per decade) but local rates of increase in NO_y may differ from this in response to circulation changes in the model via changes in the conserved tracer.

Results used in this paper come from a 45 year integration of UMETRAC (1975 to 2019), with the first five years used as model spinup. The IS92a IPCC scenario was used to determine greenhouse gas concentrations (CO_2, CH_4 and N_2O). Halogen concentrations were taken from the WMO (1999) assessment. Observed sea surface temperatures (SST) were used in the model from 1975 to 1999. For years after 1999, sea surface temperature data were taken from simulations of a coupled ocean-atmosphere

version of the UM.

Global fields of the 15 chemical tracers, 6 long-lived species and chemical families and temperature are output from UMETRAC every five days at 00:00 UT. These data are used as input for the UMETRAC column model which produced NO_2 profiles.

4.2. UMETRAC column model

The column model was used to determine the partitioning amongst the chemical families output from the full three-dimensional model. Vertical profiles of chemical families and temperature for the grid boxes covering Lauder and Arrival Heights were extracted from UMETRAC. and used as initial conditions in the column model. The chemistry scheme within the column model is identical to the chemical scheme used in the full three-dimensional model.

The column model was run for one day to establish the NO_2 diurnal cycle. The chemical time step was reduced from 15 min in the full three-dimensional model to 3 min for the column model. This allows NO_2 profiles to be calculated with a SZA resolution of 1°, ensuring the diurnal cycle of the model is adequately represented in the radiative transfer model for the calculation of slant column densities.

Finally, the NO_2 profiles calculated by the column model were interpolated from terrain following model levels to altitude surfaces from the ground to 72 km in 500 m steps.

4.3. Radiative transfer model

In transforming the measured NO_2 slant column densities to vertical column densities, some prior knowledge of the vertical profile shape is required (McKenzie et al., 1991). Assuming a vertical profile shape in an air mass factor calculation can lead to errors due to the seasonal and annual variation of the true vertical profile, which the assumed profile shape may not capture. In this work we calculated the slant column densities using the radiative transfer model developed by Schofield et al. (2003) from the profiles determined by UMETRAC. This allows direct comparison of slant column densities

derived from UMETRAC output with observations.

The RTM constructs a model atmosphere using temperature, pressure and ozone profiles taken from the UMETRAC column model. The RTM uses a spherically curved atmospheric geometry, divided into discrete atmospheric shells. For this study, ninety 1km thick shells were used to describe the model atmosphere. The effects of refraction, Rayleigh scattering, Mie scattering and molecular absorption at a wavelength of 450 nm were included in the RTM path description of the NO_2 zenith-sky measurement. Refractive indices were take from Bucholtz (1995). A single scattering approximation was used for the zenith-sky viewing geometry.

The diurnal variation of the NO_2 profile adds complexity to the slant column density calculation. The variation of the NO_2 abundance along the slant path with solar zenith angle is explicitly taken into account. NO_2 profiles at $1°$ solar zenith angle intervals between $30°$ and $97°$ calculated by the UMETRAC column model were used to construct a two-dimensional profile grid. This was then interpolated to the relevant altitude and solar zenith angle along each scattered light path. The slant column for the solar zenith angle of $90°$ was calculated by integrating the amount of NO_2 over all light paths scattered from the zenith.

5. Discussion of Lauder results

5.1. Lauder NO_2 time-series

The time-series of modelled and measured NO_2 slant column densities for Lauder are shown in Fig. 1. The model results capture the absolute value of the NO_2 slant columns and the amplitudes of the seasonal cycle in NO_2 for both sunrise and sunset very well. The model in general underestimates the observed slant columns for both the sunrise and sunset time-series. The agreement for the sunset case is somewhat worse than the sunrise which implies that the model has a suppressed NO_2 diurnal cycle.

The right hand panels of Fig. 1 show a subset of the data to illustrate more clearly the

Past and future NO$_2$

H. Struthers et al.

Title Page

Abstract	Introduction
Conclusions	References
Tables	Figures

◀ | ▶|

◀ | ▶

Back | Close

Full Screen / Esc

Print Version

Interactive Discussion

data frequency and estimated errors. The time period (August and September 1988) was chosen as representative of the whole data record, excluding the time periods affected by the El Chichon and Pinatubo eruptions. Observation errors are estimated at 0.2×10^{16} molec cm^{-2} + 5% of the observed value. This prescription comes from an analysis of the error characteristics of the measured spectra and the retrieval algorithm used to derive the NO_2 slant column measurements.

The regression model used to fit the time-series requires an error estimate associated with each input data point. In the absence of an ab initio estimate of the error in the model NO_2 slant column densities, errors are prescribed using the same error estimate as that used for the observations.

The observed data and model results from Fig. 1 were re-sampled to produce new time-series in which values were only retained for a given day, if both modelled and observed slant columns were present on that day. This processing removes sampling biases when comparing modelled and observed time-series. Figure 2 shows these time-series, with the mean annual cycles removed to show more clearly factors influencing the variability in the data. For clarity, the observation and model time-series are offset by +3 and –3 ($\times 10^{16}$ molec cm^{-2}), respectively.

The observed time-series in Fig. 2 clearly show the reduction in NO_2 amounts following the Pinatubo eruption. This effect is also seen to a lesser extent for the El Chichon eruption (1982). This reduction in NO_2 occurs via the hydrolysis of N_2O_5 to HNO_3 on the volcanic sulphate aerosol (Rodriguez et al., 1991). N_2O_5 is an important night-time NO_x reservoir and therefore removal of stratospheric N_2O_5 causes denoxification of the stratosphere. Other interannual variability is evident in the observational record. In contrast the model results show little variation other than the short term daily variability and a linear trend.

The right hand panels of Fig. 2 show the mean annual cycles for the four Lauder datasets. As indicated above, the model slant columns underestimate the observed data with the sunrise comparison being in better agreement than the sunset case. For both cases the amplitude of the modelled mean annual cycle is consistent with observations

with the whole cycle offset lower (by approximately 1×10^{16} molec cm^{-2} for sunrise and 2×10^{16} molec cm^{-2} for sunset). A constant shift of the modelled mean seasonal cycle NO$_2$ relative to observations suggests that too little NO$_y$ is present in the model. This does not explain the suppression of the diurnal cycle. More work is required to fully explain the differences between the modelled and observed mean annual cycles.

5.2. Lauder past trends and factors affecting them

Seasonally independent linear trends in the observation and model time-series, calculated using the least squares analysis algorithm are given in Fig. 3.

The NO$_2$ trends derived from observations differ from the results of Liley et al. (2000) (5% per decade) even though the same observational data-set was used in both analyses. This is because different time periods were used in the two analyses (Liley et al. (2000) studied the period 1981–1999). The 26 parameter model with autocorrelation (AC) correction used by Liley et al. (2000) for the period 1981–1999 most closely resembles the regression model used in this study. Applying our regression model to the Lauder measurements for the period 1981–1999 gives linear NO$_2$ trends that agree with the results of Liley et al. (2000).

The model NO$_2$ results underestimate the NO$_2$ trends derived from the measurements for both sunrise and sunset but the model and observed trends do agree within the 2σ uncertainty range. The trends derived from observations are significantly higher than the observed trends in N$_2$O (assumed to be between 2.5 and 3.3% per decade). This result is in agreement with the conclusions of Liley et al. (2000). The model results show a significant difference (at the 2σ level) in the NO$_2$ and N$_2$O trends for the sunset case only. The NO$_2$ results from Fig. 3 indicate that UMETRAC is not fully capturing the magnitude of the change in relative amounts of NO$_2$ and N$_2$O seen in the observations over the period 1980 to 2000. This will be discussed more fully in Sect. 5.2.1 where the seasonally dependent NO$_2$ trends are examined.

Fish et al. (2000) and McLinden et al. (2001) both show that modelled NO$_2$ trends

Past and future NO$_2$

H. Struthers et al.

Title Page

Abstract	Introduction
Conclusions	References
Tables	Figures

◄ | ►

◄ | ►

Back | Close

Full Screen / Esc

Print Version

Interactive Discussion

are sensitive to changes in ozone and temperature. Fish et al. (2000) suggest this is primarily due to the reaction,

$$NO_2 + O_3 \rightarrow NO_3 + O_2, \tag{R6}$$

which has a strong temperature dependence. To have confidence in the modelled NO_2 trends it is therefore important for the model to reproduce observed ozone and temperature trends. The model slightly overestimates the seasonally independent negative ozone trend (see Fig. 3) although the difference from observations is within the 2σ uncertainty range. Temperature trends agree well with both the observations and model showing a small negative 20 hPa temperature trend. Both the observed and modelled temperature trends are not significantly different from zero at the 2σ level.

The NO_y chemical family and HNO_3 are relatively long lived tracers in the lower stratosphere (Brasseur and Solomon, 1986). Therefore their concentrations can be influenced by both circulation changes and in-situ chemical processing. The concentrations of these species in turn control the concentration of NO_2. To further investigate the role these species have in determining trends in NO_2 in the model, NO_y and HNO_3 vertical column densities (vcds) were calculated from the model output. Every five days NO_y and HNO_3 vertical column densities were taken from the model output and the regression model applied to these time-series to determine linear trends for the period 1980–2000.

Modelled NO_y and HNO_3 seasonally independent trends at Lauder for the period 1980–2000 were calculated to be +2.5±1.1% per decade and +1.8±1.3% per decade, respectively (Table 1). The 2.5% per decade trend in NO_y matches the global rate of increase in N_2O and is significantly less than the observed trends in NO_2.

The fact that HNO_3 is increasing at a lower rate than NO_y suggests that the higher trend in NO_2 over the period 1980–2000 is gained at the expense of HNO_3, and therefore the partitioning in NO_y over this period is shifting towards the more chemically active NO_x species and away from the HNO_3 reservoir. Additional analysis is required to determine what fraction of the difference between the NO_y and HNO_3 trends can be

Title Page

Abstract | Introduction

Conclusions | References

Tables | Figures

◄ | ►►

◄ | ►

Back | Close

Full Screen / Esc

Print Version

Interactive Discussion

attributed to circulation changes and what fraction of the difference is due to chemical forcing.

5.2.1. Annually varying NO_2 trends

Figure 4 shows the seasonally dependent NO_2 trends calculated by adding two Fourier
5   components (annual and semi-annual) to the basis function describing the trend in the regression model (Bodeker et al., 1998). The trends are taken as a percentage of the daily mean. That is, the trends are calculated in units of molec cm^{-2} per decade and then taken as a percentage of the annual mean over the whole period (given in the right hand panels of Fig. 2).
10   The results shown in Fig. 4 indicate that for much of the year, the model NO_2 trends are in good agreement with the trends derived from observations. The greatest differences occur in spring time for both sunrise and sunset cases, where the model is underestimating the trends seen in the observations. The model underestimation of the springtime increase in NO_2 is the cause of the model failing to fully reproduce the
15   difference between the seasonally independent NO_2 and N_2O trends for the period 1980 to 2000 (see Fig. 3).
     The same regression model (with seasonally dependent basis functions for the linear trend term) was used to fit the modelled and measured ozone and 20 hPa temperature time-series. The seasonal cycle in ozone and 20 hPa temperature trends was repro-
20   duced well by the model (not shown). Therefore ozone and temperature were ruled out as the cause of the model underprediction of springtime NO_2 trends.
     Differences in the timing of the vortex breakup and subsequent mixing of vortex and mid-latitude air can also be ruled out as the cause of the differences in the modelled and observed Lauder springtime NO_2 trends. Generally, the mixing of vortex air to
25   mid-latitudes occurs in early summer (Ajtic, 2004), from approximately day 288 (15 October) which is after the maximum in the trend differences (approximately day 240 – 28 August). The model, if anything, tends to delay the breakup of the Antarctic polar vortex further reinforcing this conclusion.

Title Page

Abstract	Introduction
Conclusions	References
Tables	Figures

|◄ | ►|
◄ | ►
Back | Close

Full Screen / Esc

Print Version

Interactive Discussion

Stratospheric NO_2 amounts have been shown to be sensitive to changes stratospheric water vapour (Fish et al., 2000; McLinden et al., 2001). Trends in stratospheric water vapour are uncertain (SPARC, 2000; Rosenlof et al., 2001) but observational records do indicate an increase of the order of 1% per year over the past 20 years. In this study, UMETRAC used a fixed climatology of stratospheric water vapour which may contribute to the discrepancy between modelled and observed NO_2 trends. Additional sensitivity tests of the model are required to diagnose the model response to changing stratospheric water vapour.

5.3. Model predictions: Lauder 2001–2019

Table 1 (and Fig. 3) compares the seasonally independent, predicted NO_2 model trends for the period 1 January 2001 to 31 December 2019 with the model trends for the period 1 January 1980 to 31 December 2000.

Predicted NO_2 trends (2001–2019) are lower than the trends for the period 1980–2000 even though the N_2O trend stays the same. This difference is statistically significant at the 2σ level for the sunset case. Both the absolute and relative differences between trends for the two periods are larger for the sunset case.

NO_y and HNO_3 vertical column density trends for the period 2001–2019 are compared with the 1980–2000 trends in Table 1. It is clear from Table 1 that the shift in NO_2 trends from 1980–2000 to 2001–2019 is associated with a change in HNO_3 trends between the two periods. As was the case for the 1980–2000 period, it is a change in partitioning of the NO_y that is resulting in the less than proportional rate of increase in NO_2 relative to NO_y (and N_2O) rather than local changes in the amount of NO_y relative to N_2O.

Quantification of how chemical changes (for example halogen loading and ozone) and circulation changes affect NO_y partitioning requires additional analysis of model results which is outside the scope of this paper.

It should be reiterated that the results shown here are for a solar zenith angle of 90°. McLinden et al. (2001) show that the trends in NO_2 vary significantly with solar

zenith angle. It is therefore to be expected that different conclusions may be drawn from analysis of data at different solar zenith angles.

6. Discussion of Arrival Heights results

6.1. Arrival Heights NO_2 time-series

5 Arrival Heights slant column density comparisons are shown in Fig. 5. Twilight (SZA = 90°) data at Arrival Heights are only available during the autumn (17 February to 21 April) and spring (22 August to 25 October). Because of the large annual cycle, daily and seasonal variability and the discontinuous nature of the data, it is difficult to assess the level of agreement in the data from Fig. 5.

10 Figure 6 shows the processed Arrival Heights time-series comparison with the annual mean removed (see Sect. 5.1 and Fig. 2). Significantly less data are available for Arrival Heights than for Lauder because of the limited period of twilight (spring and autumn) at Arrival Heights and gaps in the observation record, particularly in the years 1982–1989. Both the observed and modelled data for Arrival Heights show greater

15 variability about the mean than the Lauder data.

There is good qualitative agreement between observations and model for the mean seasonal cycle at both sunrise and sunset. However, during autumn, the model tends to systematically underpredict the observations, possibly for reasons discussed in Sect. 7.

20 ### 6.2. Arrival Heights NO_2 trends

Regression analysis of the Arrival Heights data is complicated by the discontinuous nature of the data. We analyse the autumn and spring data separately as the chemical and dynamical regimes during the two seasons are markedly different and therefore the NO_2 response is expected to be different for the two seasons. No seasonal com-

ponents were included as part of any of the basis functions used in the regression model.

The basis function describing the effect of the El Chichon eruption was not used in the regression analysis of the Arrival Heights data because the first observation available is 30 August 1982, approximately five months after the El Chichon eruption. The El Chichon basis function would include only a decay term and can potentially induce spurious trend results if included.

Because the NO_2 slant columns are correlated with 20 hPa temperature, particularly in the spring, an additional basis function was added to the regression model which describes the 20 hPa temperature. This allows the regression model to fit anomalous NO_2 slant columns associated with anomalous 20 hPa temperatures. The temperature basis function was generated by taking daily Arrival Heights 20 hPa temperatures from the NCEP/NCAR reanalysis data-set and fitting them using the same regression model as is used for the NO_2 data. The residual temperatures from this fitting were then used as the temperature basis function for the regression analysis of the NO_2 data. The same process was applied to the model 20 hPa temperatures to generate the model temperature basis function.

Figure 7 gives the linear, seasonal (autumn and spring) trends in NO_2, N_2O, ozone and temperature for Arrival Heights from the model and observations for the period September 1982 to October 2000. It is evident from this figure that the 2σ uncertainties in the derived trends for both the observations and model are large compared to the trends themselves. Although there is agreement between modelled and observed trends for all cases it is difficult to attribute any significance to the comparison given the large uncertainties.

Modelled and observed autumn NO_2 trends are greater than the spring NO_2 trends. It is expected that increases in NO_y and NO_2 in the springtime polar regions will be offset to some extent by denitrification (and denoxification) of the lower stratosphere which is implied by these results but the amounts have not been quantified. As is the case with the Lauder comparison, the model underpredicts the rate of increase in NO_2

◄◄ | ►►

◄ | ►

Back | Close

Full Screen / Esc

Print Version

Interactive Discussion

relative to the observations in all cases.

The autumn NO_2 trends shown in Fig. 7 are similar to the Lauder results from Fig. 3. The ozone and 20 hPa temperature results are also similar. Thus, at high latitudes in autumn, the stratosphere is showing a similar response in NO_2, ozone and temperature to mid-latitudes. This is expected given the quiescent and well mixed nature of the summer and autumn extratropical stratosphere.

The chemically and dynamically disturbed high latitude spring on the other hand, shows some deviations from previous results. As expected, the negative ozone trends are significantly larger than the autumn case and as mentioned previously, the NO_2 trends are closer to the N_2O trends than for autumn.

6.3. Model predictions: Arrival Heights 2000–2019

The predicted (2001–2019) NO_2, ozone and temperature trends for Arrival Heights are shown in Table 2 and Fig. 7. As with the autumn model/observation comparison discussed in the previous section, the autumn model predictions are similar to the Lauder results (see Table 1). NO_2 increases at a greater than equivalent rate with respect to N_2O for the period 1982–2000. This is followed by a shift to a less than equivalent increase in NO_2 for 2001–2019. The change in NO_2 trends is associated with a change in ozone trends from a negative trend of −4.1% per decade to a small positive trend (+1.9±4.3% per decade).

Spring NO_2 trends for both the 1982–2000 period and the 2001–2019 period are close to the N_2O trend applied to the model. There is a small decrease in the 2001–2019 predicted trends relative to the 1982–2000 results but the difference is less than the autumn case. The large change in model ozone trends (−13.7±16.6% per decade to +1.0±11.0% per decade) in this case is not associated with a significant change in NO_2 trends.

Table 2 gives the autumn and spring NO_y and HNO_3 vertical column trends derived from Arrival Heights model output. HNO_3 trends follow a similar pattern to the Lauder data (see Table 1), with a change from low values for 1982–2000 to higher values for

the 2001–2019 period, the change in HNO_3 trends being mirrored by the changes in NO_2 trends.

A problem with this picture arises in the autumn data, where the predicted trend in NO_y is 5.4% per decade, approximately equal to the HNO_3 trend of 5.2% per decade. If NO_y and HNO_3 trends only were controlling the NO_2 trends, then the predicted NO_2 trend would also be expected to be close to 5.4% per decade, rather than approximately 1% per decade as predicted by the model.

It is clearly important to try and reduce the uncertainty associated with the regression model's estimates of linear trends from the Arrival Heights data. At this time, the large level of uncertainty means no significant conclusions can be drawn from the Arrival Heights data. A more thorough investigation of the sources of variability in the Arrival Heights data is required.

7.   Conclusions

7.1.   Lauder

Model slant column densities compare well with the measured 90° slant columns. Both the annual cycle and diurnal cycle are reproduced by the model. Systematic underprediction of the measurements by the model is most likely due to an underprediction of the amount of NO_y. Although this affects the absolute values of the NO_2 slant columns, the percentage trends from the model are not directly affected by any mis-specification of the NO_y amounts.

Modeled and measured linear trends for the period 1980–2000 agree within the 2σ uncertainty range, for both the sunrise and sunset cases. Both the model and measurements show a greater rate of increase of NO_2 compared with N_2O suggesting a change in the partitioning of the oxides of nitrogen over Lauder. Model NO_y and HNO_3 trends over the same period confirm that, in the model, there is a change in partitioning of the NO_y family from the reservoir HNO_3 to the more chemically active NO_x species.

Past and future NO$_2$

H. Struthers et al.

◄◄   ►►

◄   ►

Back   Close

Full Screen / Esc

Print Version

Interactive Discussion

The largest discrepancy between modeled and measured NO_2 trends occurs in springtime when model NO_2 trends are lower than the trends derived from measurements for both sunrise and sunset cases. The annually varying trends still agree at the 2σ level. It is not clear at this time what is causing the model to underpredict the NO_2 trends during this time of the year. Polar vortex air mixing into mid-latitudes does not occur until early summer which rules out vortex air being the cause. Failure of the model to capture changes in chemistry or dynamics or both could explain the discrepancy in NO_2 trends.

Significant changes in the rate of increase of NO_2 (at a SZA of 90°) are predicted by the model for the period 2001–2019 compared with the period 1980–2000. Trends in NO_2 are greater than the trends in N_2O (and NO_y) for the period 1980–2000 with a reverse for the period 2001–2019. Changes in the NO_2 trends are associated with changes in HNO_3 trends, the ratios NO_x/NO_y and HNO_3/NO_y being anticorrelated.

Concurrent changes in ozone and stratospheric halogen trends are also found in the model results when comparing the 1980–2000 period with 2001–2019 but without additional sensitivity experiments it is not possible to fully determine the nature of the coupling between the NO_y partitioning and other variables within the model.

7.2. Arrival Heights

As was the case with the Lauder comparison, the model results at Arrival Heights reproduce well the measured seasonal and diurnal cycles of NO_2 slant column densities at sunrise and sunset. Autumn model results consistently underestimate the measured values. The most likely reason for this is an underestimation of the amount of NO_y in the model during this season.

Large variability in both the measured and modeled slant column densities result in large estimates in the errors of the trends in NO_2, ozone and temperature relative to the trends themselves. This makes interpretation of the trend results difficult and care must be taken in assigning significance to the conclusions drawn.

Autumn trend results for Arrival Heights are similar to the annually averaged results

Past and future NO$_2$

H. Struthers et al.

Title Page

Abstract | Introduction

Conclusions | References

Tables | Figures

◄ | ►►

◄ | ►

Back | Close

Full Screen / Esc

Print Version

Interactive Discussion

from Lauder. NO_2 increases at a faster rate than N_2O (and NO_y in the model) for the period 1980–2000, followed by a decrease in the NO_2 trends for the 2001–2019 period. Modeled HNO_3 indicates that the partitioning of NO_y follows a similar course to the Lauder results with an increase in the relative amount of NO_x at the expense of HNO_3 up to approximately the year 2000. This change is reversed in the model for the period 2001–2019.

For the chemically and dynamically active Antarctic spring, secular changes in NO_y partitioning are less pronounced. NO_2, HNO_3 and N_2O (NO_y) trends are all similar over the whole period of the integration. Denitrification of the polar stratosphere is an important process which occurs during the winter/spring period and is expected to significantly influence the trends in the oxides of nitrogen over Arrival Heights during spring. Currently the model uses a simple NAT/ice sedimentation scheme using a fixed sedimentation velocity as thus are not expected to capture the full detail of this process.

References

Ajtic, J., Connor, B., Lawerence, B., Bodeker, G., Hoppel, K., Rosenfield, J., and Heuff, D.: Dilution of the Antarctic ozone hole into southern midlatitudes: 1998–2000, J. Geophys. Res., accepted, 2004. 4560

Austin, J.: On the explicit versus family solution of the fully diurnal photochemical equations of the stratosphere, J. Geophys. Res., 96, 12 941–12 974, 1991. 4553

Austin, J. and Butchart, N.: Coupled chemistry-climate model simulations for the period 1980-2020: Ozone depletion and the start of the ozone recovery, Q. J. R. Meteorol. Soc., 129, 3225–3249, 2003. 4554

Past and future NO$_2$

H. Struthers et al.

Bodeker, G., Boyd, I., and Matthews, W.: Trends and variability in vertical ozone and temperature profiles measured by ozonesondes as Lauder, New Zealand: 1986-1996, J. Geophys. Res., 103, 28 661–28 681, 1998. 4552, 4553, 4560

Bodeker, G., Scott, J., Kreher, K., and McKenzie, R.: Global ozone trends in potential vorticity coordinates using TOMS and GOME intercompared against the Dobson network: 1978–1998, J. Geophys. Res., 106, 23 029–23 042, 2001. 4552

Brasseur, G. and Solomon, S.: Aeronomy of the middle atmosphere, D. Reidel Publishing Company, Dordrecht, The Netherlands, second edn., 1986. 4559

Bucholtz, A.: Rayleigh-scattering calculations for the terrestrial atmosphere, Applied Optics, 34, 2765–2773, 1995. 4556

Crutzen, P.: The influence of nitrogen oxides on the atmospheric ozone content, Q. J. R. Meteorol. Soc., 96, 320–325, 1970. 4546

Cullen, M. and Davies, T.: Conservative split-explicit integration scheme with fourth-order horizontal advection, Q. J. R. Meteorol. Soc., 117, 993–1002, 1991. 4553

DeMore, W., Sander, S., Golden, D., Hampson, R., Kurylo, M., Howard, C., Ravishankara, A., Kolb, D., and Molina, M.: Chemical kinetics and photochemical data for use in stratospheric modelling, Tech. Rep. Evaluation number 12, Pasadena, Ca, 1997. 4554

Fish, D., Roscoe, H., and Johnston, P.: Possible causes of stratospheric NO_2 trends observed at Lauder, New Zealand, Geophys. Res. Lett., 27, 3313–3316, 2000. 4549, 4550, 4551, 4558, 4559, 4561

Grainger, J. and Ring, J.: Lunar luminescence and solar radiation, Space Res., 3, 989, 1963. 4551

IPCC: IPCC, Climate Change 2001: The Scientific Basis, Contribution of Working Group 1 to the Third Assessment Report of the Intergovernmental Panel on Climate Change, Tech. rep., Cambridge, UK, 2001. 4547

Johnston, P. and McKenzie, R.: NO_2 observations at 45° S during the decreasing phase of solar cycle 21, from 1980 to 1987, J. Geophys. Res., 94, 3473–3486, 1989. 4548, 4551

Kalnay, E., Kanamitsu, M., Kistler, R., Collins, W., Deaven, D., Gandin, L., Iredell, M., Saha, S., White, G., Woollen, J., Zhu, Y., Leetmaa, A., Reynolds, R., M.Chelliah, Ebisuzaki, W., Higgins, W., Janowiak, J., Mo, K. C., Ropelewski, C., Wang, J., Jenne, R., and Joseph, D.: The NCEP/NCAR 40-year reanalysis project, Bull. Am. Meteorol. Soc., 77, 437–471, 1996. 4552

Keys, J. and Johnston, P.: Stratospheric NO_2 and O_3 in Antarctica: Dynamic and chemically

© EGU 2004

controlled variations, Geophys. Res. Lett., 13, 1260–1263, 1986. 4549, 4552

Keys, J. and Johnston, P.: Stratospheric NO$_2$ column measurements for three Antarctic sites, Geophys. Res. Lett., 15, 898–900, 1988. 4549

Liley, J., Johnston, P., McKenzie, R., Thomas, A., and Boyd, I.: Stratospheric NO$_2$ variations from a long time series at Lauder, New Zealand, J. Geophys. Res., 105, 11 633–11 640, 2000. 4549, 4551, 4558

McKenzie, R. and Johnston, P.: Springtime stratospheric NO$_2$ in Antarctica, Geophys. Res. Lett., 11, 73–75, 1984. 4549

McKenzie, R., Johnston, P., McElroy, C., Kerr, J., and Solomon, S.: Altitude distributions of stratospheric constitutuents from ground-based measurements at twilight, J. Geophys. Res., 96, 15 499–15 511, 1991. 4555

McLinden, C., Olsen, S., Prather, M., and Liley, J. B.: Understanding trends in stratospheric NO$_y$ and NO$_2$, J. Geophys. Res., 106, 27 787–27 793, 2001. 4550, 4551, 4558, 4561

Minschwener, K., Salawitch, R., and McElroy, M.: Absorption of solar radiation by O$_2$: Implications for O$_3$ and lifetimes of N$_2$O, CFCl$_3$ and CF$_2$Cl$_2$, J. Geophys. Res., 98, 10 543–10 561, 1993. 4547

Plumb, R. and Ko., M. K. W.: Interrelationships between mixing ratios of long-lived stratospheric constituents, J. Geophys. Res., 99, 10 145–10 156, 1992. 4554

Randeniya, L., Vohralik, P., Plumb., I., and Ryan, K. R.: Heterogeneous BrONO$_2$ hydrolysis: Effect on NO$_2$ columns and ozone at high latitudes in summer, J. Geophys. Res., 102, 23 543–23 557, 1997. 4547

Randeniya, L., Vohralik, P., and Plumb, I.: Stratospheric ozone depletion at northern mid latitudes in the 21st century: The importance of future concentrations of greenhouse gases nitrous oxide and methane, Geophys. Res. Lett., 29, doi:10.1029/2001GL014 295, 2002. 4547, 4548

Rinsland, C., Weisenstein, D., Ko, M. K. W., Scott, C., Chiou, L., Mahein, E., Zander, R., and Demoulin, P.: Post-Mount Pinatubo eruption ground-based measurements of HNO$_3$, NO and NO$_2$ and their comparison with model calculations, J. Geophys. Res., 108, doi:10.1029/2002JD002 965, 2003. 4549

Rodriguez, J., Ko, M. K. W., and Sze, N.-D.: Role of heterogeneous conversion of N$_2$O$_5$ on sulphate aerosols in global ozone losses, Nature, 352, 134–137, 1991. 4557

Rosenlof, K., Oltmans, S., Kley, D., Russell, J., Chiou, E.-W., Chu, W., Johnson, D., Kelly, K., Michelsen, H., Nedoluha, G., Remsberg, E., Toon, G., and McCormick, M.: Stratospheric

water vapour increases over the past half-century, Geophys. Res. Lett., 28, 1195–1198, 2001. 4561

Sander, S., Ravishankara, A., Friedl, R., DeMore, W., Golden, D., Kolb, C., Kurylo, M., Molina, M., Hampson, R., Huie, R., and Moortgat, G.: Chemical kinetics and photochemical data for use in stratospheric modelling, Tech. Rep. Evaluation number 12: Update of key reactions, Pasadena, Ca, 2000. 4554

Scaife, A., Butchart, N., Warner, C., Stainforth, D., Norton, W., and Austin, J.: Realistic quasi-biennial oscillations in a simulation of the global climate, Geophys. Res. Lett., 27, 3481–3484, 2000. 4553

Schofield, R., Connor, B. J., Kreher, K., Johnston, P., and Rodgers, C.: The retrieval of profile and chemical information from ground-based UV-Visible spectroscopic measurements, J. Quantitative Spectroscopy and Radiative Transfer, 86, 115–131, 2003. 4555

Solomon, S., Schmeltekopf, A., and Saunders, R.: On the interpretation of zenith sky absorption measurements, J. Geophys. Res., 92, 8311–8319, 1987. 4549

SPARC: 2000: SPARC assessment of upper tropospheric and stratospheric water vapour, Tech. Rep. WMO-TD No. 1043, WCRP Series Report No. 113, SPARC Report No. 2, Berrieres le Buisson Cedex, http://www.aero.jussieu.fr/~sparc/WAVASFINAL_000206/ WWW_wavas/WavasComplet.pdf, 2000. 4561

Warner, C. and McIntyre, M.: Toward an ultra simple spectral gravity wave parameterization for general circulation models, Earth Planets Space, 51, 475–484, 1999. 4553

WMO: Scientific Assessment of Ozone Depletion: 1991, WMO Global Ozone Research and Monitoring Project, Tech. Rep. Report No. 25, Geneva, Switzerland, 1991. 4554

WMO: Scientific Assessment of Ozone Depletion: 1998, WMO Global Ozone Research and Monitoring Project, Tech. Rep. Report No. 44, Geneva, Switzerland, 1999. 4547, 4549, 4554

WMO: Scientific Assessment of Ozone Depletion: 2002, WMO Global Ozone Research and Monitoring Project, Tech. Rep. Report No. 47, Geneva, Switzerland, 2003. 4547, 4548, 4549

Zander, R., Ehhalt, D., Rinsland, C., Schmidt, U., Mahieu, E., Rudolph, J., Demoulin, P., Roland, G., Delbouille, L., and Sauval, A.: Secular trend and seasonal variability of the column abundance of N_2O above the Jungfraujoch station determined from IR spectra, J. Geophys. Res., 99, 16 745–16 756, 1994. 4547

Past and future NO$_2$

H. Struthers et al.

Title Page

Abstract	Introduction
Conclusions	References
Tables	Figures

◄◄ | ►►

◄ | ►

Back | Close

Full Screen / Esc

Print Version

Interactive Discussion

Table 1. Lauder – seasonally independent UMETRAC model trends in NO$_2$, N$_2$O, ozone, temperature, NO$_y$ and HNO$_3$ for the periods 1981–2000 and 2001–2019. Trends are given in percent per decade (temperature trends are shown in K/decade). The quoted errors are ±2σ.

	Model (1981–2000)		Model (2001–2019)	
	am	pm	am	pm
NO$_2$	4.2±1.8	3.9 ±1.2	2.2±1.8	0.97±1.4
N$_2$O	2.6		2.6	
Ozone	−3.3±0.7		1.3±0.9	
Temperature	−0.16±0.15		−0.17±0.20	
NO$_y$	2.5±1.1		2.7±1.3	
HNO$_3$	1.8±1.3		3.3±1.5	

ACPD

4, 4545–4579, 2004

Past and future NO$_2$

H. Struthers et al.

Title Page

Abstract | Introduction

Conclusions | References

Tables | Figures

◄◄ | ►►

◄ | ►

Back | Close

Full Screen / Esc

Print Version

Interactive Discussion

© EGU 2004

Table 2. Autumn and spring trends in NO$_2$, N$_2$O, ozone, temperature, NO$_y$ and HNO$_3$ derived from model results for Arrival Heights for the periods 1982–2000 and 2001–2019. Trends are given in % per decade (temperature trends are shown in K/decade). The quoted errors are ±2σ.

	Autumn				Spring			
	Model (1982–2000)		Model (2001–2019)		Model (1982–2000)		Model (2001–2019)	
	am	pm	am	pm	am	pm	am	pm
NO$_2$	4.7±7.5	3.9±8.9	1.0±7.4	1.2±8.0	3.0±4.0	2.7±4.4	2.1±3.0	1.6±3.2
N$_2$O	2.6		2.6		2.6		2.6	
Ozone	−4.1±4.6		1.9±4.3		−13.7±12.6		1.0±11.0	
Temperature	0.3±0.5		0.0±0.72		−0.4±3.2		−0.5±4.5	
NO$_y$	2.3±5.0		5.4±7.6		4.6±4.0		3.0±7.6	
HNO$_3$	1.2±3.2		5.2±4.1		−0.6±4.6		6.0±5.1	

Past and future NO$_2$

H. Struthers et al.
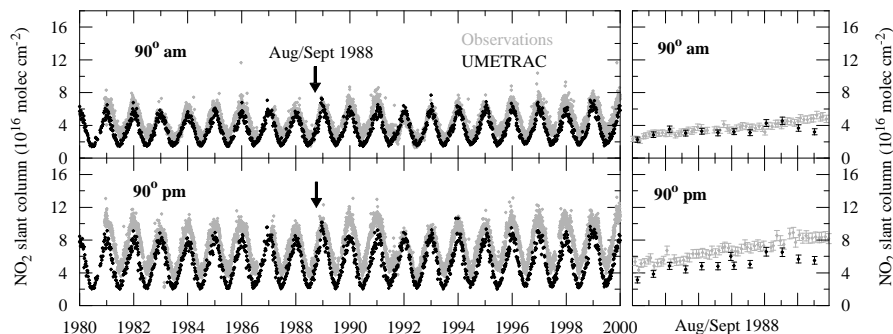
Fig. 1. Comparison of UMETRAC modelled (black) and observed (grey) 90° NO$_2$ slant column density time-series for Lauder (1980–2000). Upper left panel sunrise, lower left panel sunset. A subset of the data is shown in the right hand panels to illustrate the estimated errors in the model and observed values and the data frequency.
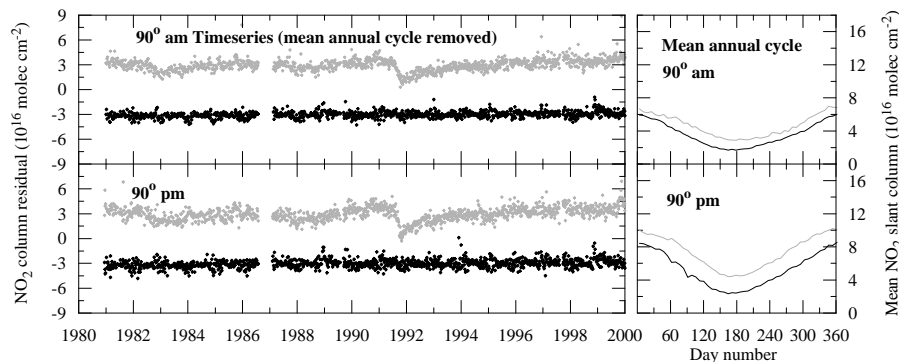
Fig. 2. Lauder NO$_2$ slant column density time-series with the mean annual cycle removed. Observed residuals (grey) have been offset by +3 units and the model residuals (black) offset by −3 units for clarity. The time-series have been thinned by retaining data only when both observation and model values are present on a given day. Right hand panels show the mean annual cycles (1980–2000) for sunrise (top) and sunset (bottom).
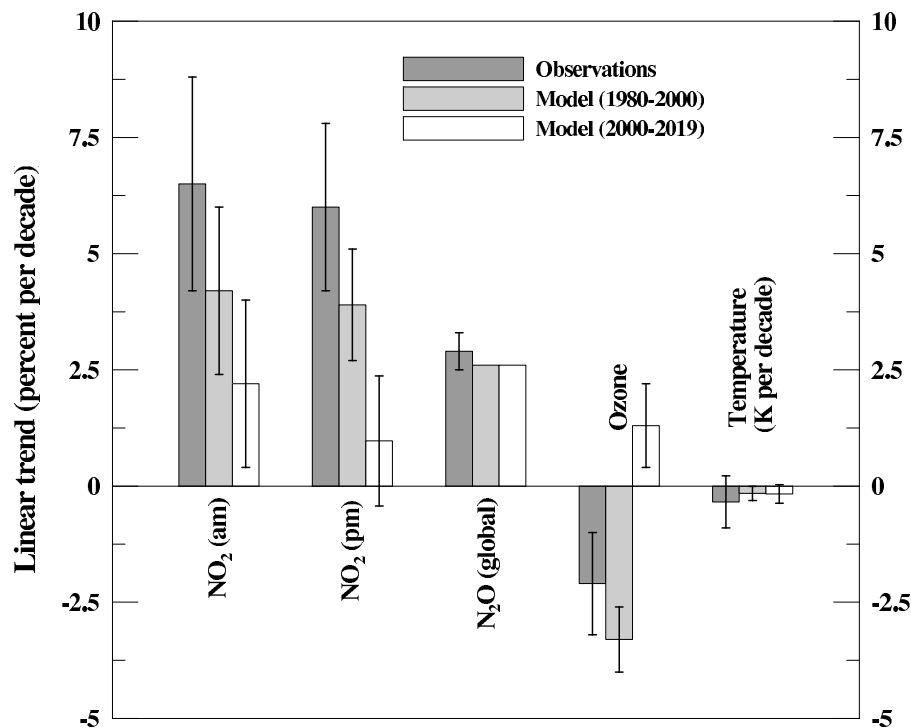
Fig. 3. Seasonally independent trends in NO$_2$ for Lauder in % per decade, derived from observations and UMETRAC model results. Also given are the estimated trends in global N$_2$O over the same time periods and the observed and modelled trends in ozone and temperature (temperature trends are shown in K/decade). The errors are ±2σ. Note, model N$_2$O trends are the prescribed global value and thus has no error associated with them.

ACPD

4, 4545–4579, 2004

Past and future NO$_2$

H. Struthers et al.

Title Page

Abstract | Introduction

Conclusions | References

Tables | Figures

◄◄ | ►►

◄ | ►

Back | Close

Full Screen / Esc

Print Version

Interactive Discussion

© EGU 2004
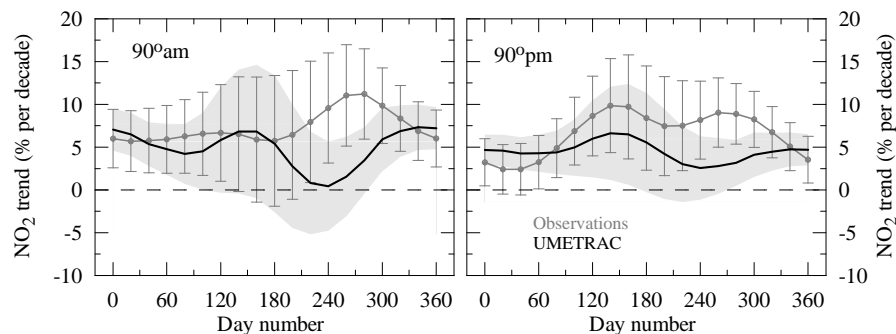
Fig. 4. Annually varying NO$_2$ trends for Lauder for the period 1980–2000. The grey shaded region represents the 2σ uncertainty range in the trends derived from model output. Error bars on the observed trends indicate ±2σ.

Past and future NO$_2$

H. Struthers et al.
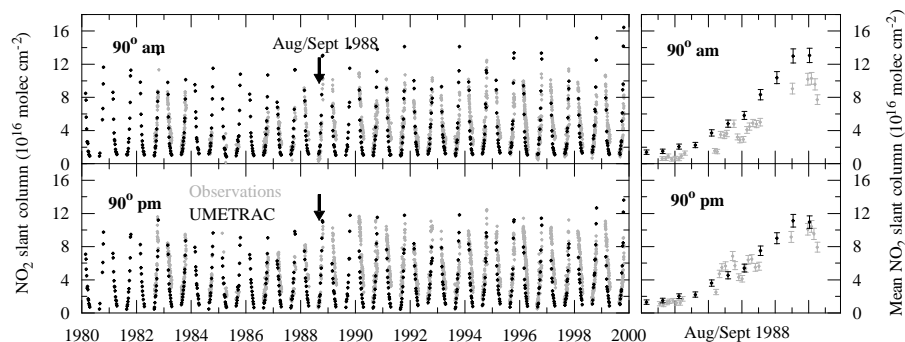
Fig. 5. Comparison of UMETRAC modelled (black) and observed (grey) 90° NO$_2$ slant column density time-series for Arrival Heights (1980–2000). Upper left panel sunrise, lower left panel sunset. A subset of the data is shown in the right hand panels to illustrate the estimated errors in the model and observed values and the data frequency.
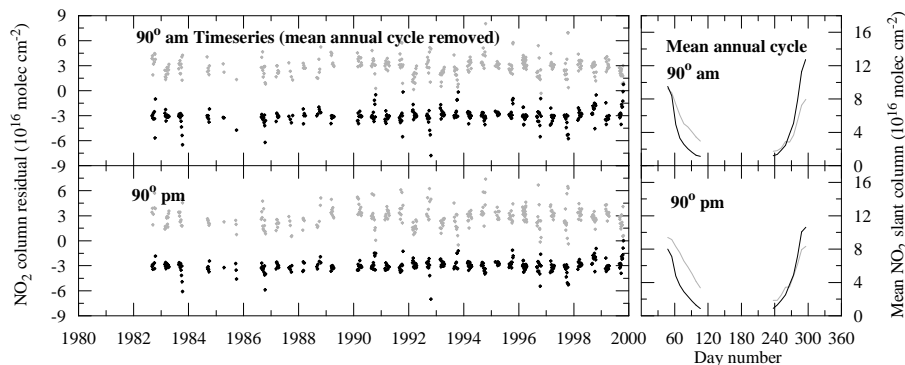
Fig. 6. Arrival Heights NO$_2$ slant column density time-series with the mean annual cycle removed. Observed residuals (grey) have been offset by +3 units and the model residuals (black) offset by −3 units for clarity. The time-series have been thinned by retaining data only when both an observation and model value is present on a given day. Right hand panels show the mean annual cycles (1980–2000) for sunrise and sunset.

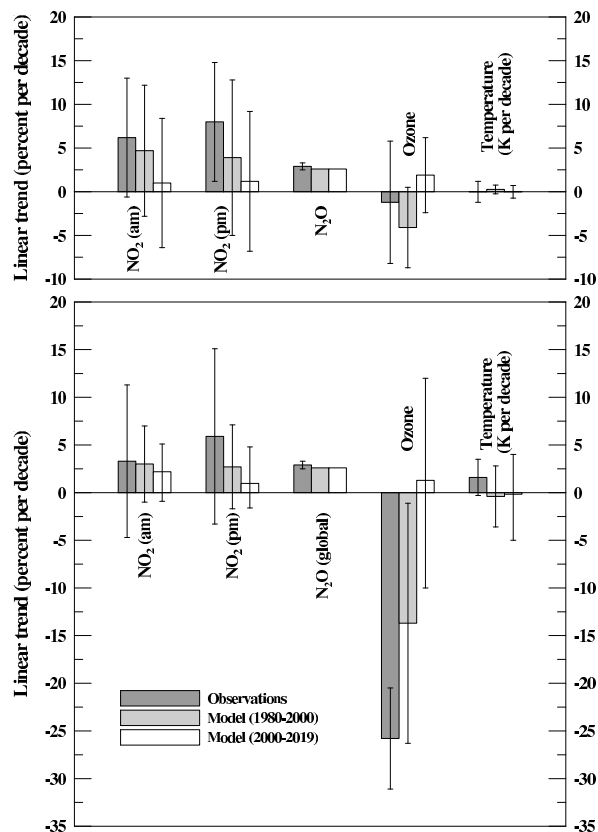**Past and future NO$_2$**

H. Struthers et al.

Fig. 7. Autumn and spring trends in NO$_2$, N$_2$O, ozone and temperature derived from observations and model results for Arrival Heights. Trends are given in % per decade (temperature trends are shown in K/decade). The errors are ±2σ.